

# Northumbria Research Link

Citation: Feng, Huijuan, Chen, Yan, Dai, Jian S. and Gogu, Grigore (2017) Kinematic study of the general plane-symmetric Bricard linkage and its bifurcation variations. Mechanism and Machine Theory, 116. pp. 89-104. ISSN 0094-114X

Published by: Elsevier

URL: <https://doi.org/10.1016/j.mechmachtheory.2017.05.019>  
<<https://doi.org/10.1016/j.mechmachtheory.2017.05.019>>

This version was downloaded from Northumbria Research Link:  
<http://nrl.northumbria.ac.uk/id/eprint/43912/>

Northumbria University has developed Northumbria Research Link (NRL) to enable users to access the University's research output. Copyright © and moral rights for items on NRL are retained by the individual author(s) and/or other copyright owners. Single copies of full items can be reproduced, displayed or performed, and given to third parties in any format or medium for personal research or study, educational, or not-for-profit purposes without prior permission or charge, provided the authors, title and full bibliographic details are given, as well as a hyperlink and/or URL to the original metadata page. The content must not be changed in any way. Full items must not be sold commercially in any format or medium without formal permission of the copyright holder. The full policy is available online: <http://nrl.northumbria.ac.uk/policies.html>

This document may differ from the final, published version of the research and has been made available online in accordance with publisher policies. To read and/or cite from the published version of the research, please visit the publisher's website (a subscription may be required.)



**Northumbria  
University**  
NEWCASTLE



**UniversityLibrary**

# Kinematic Study of the General Plane-symmetric Bricard Linkage and Its Bifurcation Variations

Huijuan Feng<sup>1,2</sup>, Yan Chen<sup>1\*</sup>, Jian S. Dai<sup>1,3</sup>, Grigore Gogu<sup>2</sup>

<sup>1</sup>Key Laboratory of Mechanism Theory and Equipment Design of Ministry of Education,  
Centre for Advanced Mechanisms and Robotics (CAMAR),  
School of Mechanical Engineering, Tianjin University, Tianjin 300072, PR China

<sup>2</sup>Université Clermont Auvergne, CNRS, SIGMA Clermont, Institut Pascal,  
F-63000 Clermont-Ferrand, France

<sup>3</sup>Center for Robotics Research, King's College London, University of London,  
Strand, London WC2R 2LS, UK

## Abstract:

In this paper, the explicit solutions to closure equations of the plane-symmetric Bricard linkage are derived and a thorough kinematic study of the general plane-symmetric Bricard linkage is conducted with DH matrix method. The derived  $5R/4R$  linkages from this Bricard linkage are introduced. Various bifurcation cases of the plane-symmetric Bricard linkage with different geometric conditions are discussed, which include the bifurcation between two plane-symmetric Bricard linkage motion branches and the bifurcation among equivalent serial kinematic chains with revolute joints and a four-bar double-rocker linkage. Especially the plane-symmetric Bricard linkage that can bifurcate to the Bennett linkage is proposed for the first time. These findings not only offer an in-depth understanding about the kinematics of the general plane-symmetric Bricard linkage, but also bridge two overconstrained linkage groups, i.e., the Bennett-based linkages and Bricard-related ones, to reveal their intrinsic relationship.

## Keywords:

Kinematics; the plane-symmetric Bricard linkage; explicit solution; closure equations; bifurcation.

## 1. Introduction

The family of  $6R$  overconstrained linkages was proposed by Bricard consists of three deformable octahedral cases [1] and three spatial linkage cases [2] whose mobility is due to the symmetric property. Among them, the plane-symmetric Bricard linkage has been extensively studied. First of all, implicit closure equations of six Bricard linkages were derived by Baker with DH loop-closure matrix method [3]. Phillips reviewed the Bricard linkages and introduced their relationship with other overconstrained linkages [4]. Baker analysed the general plane-symmetric six-screw linkage including the plane-symmetric Bricard linkage with the reciprocal screw system approach [5]. The movability of the plane-symmetric Bricard linkage was investigated by Li and Schicho based on the theory of bonds [6]. Deng *et al* presented a geometric approach for design

---

\* Corresponding author.

E-mail address: [yan\\_chen@tju.edu.cn](mailto:yan_chen@tju.edu.cn)

and synthesis of single loop mechanisms including the plane-symmetric Bricard linkage [7]. They also proposed a virtual chain approach for the mobility analysis of multi-loop deployable mechanisms with plane-symmetric Bricard linkage as basic element [8]. Kong conducted type synthesis of single-loop overconstrained  $6R$  spatial mechanisms for circular translation in which the plane-symmetric Bricard linkage is taken as an example [9]. Even though various synthesis methods have been used to study the plane-symmetric Bricard linkage, there is no progress on the explicit solution of closure equations after Baker's implicit ones. The detailed kinematic behaviours of this linkage can be revealed only with the explicit solutions. Therefore, we set the target to obtain them by overcoming the complicated trigonometric functions.

Recent research applies the plane-symmetric Bricard linkage to the design of deployable structures. For example, Chen *et al* proposed a threefold-symmetric Bricard linkage which is a special case of the plane-symmetric one to fold the triangular or hexagonal structures [10]. Viquerat *et al* design a rectangular ring which can be folded into a compact bundle. Kinematically this is an alternative form of the plane-symmetric Bricard linkage [11]. A number of such retractable rectangular rings can form a family of large deployable mechanisms by synchronising the motion of all linkages [12].

Because of the symmetry property, the plane-symmetric Bricard  $6R$  linkage tends to have complicated bifurcation behaviours, which should be avoided in the application of deployable structures, but could be made use of in the design of reconfigurable mechanisms. The kinematics and bifurcation behavior of a special line- and plane-symmetric Bricard linkage was analyzed using the SVD numerical method by Chen and Chai [13]. Zhang and Dai analyzed motion branch variations of the line- and plane-symmetric Bricard linkage based on reciprocal screw systems [14]. Recent work on thick-panel origami shows 6-crease origami pattern can be replaced with the plane-symmetric Bricard linkage in the thick-panel model [15]. Moreover, the kinematic model of the thick-panel waterbomb origami is the assembly of two types of plane-symmetric Bricard linkages with bifurcation under certain geometric conditions [16]. Hence, the current bifurcation analysis of the plane-symmetric Bricard linkage only focuses on special cases. Therefore, this paper also aims to setup the general geometric condition of the bifurcation for the plane-symmetric Bricard linkage.

The layout of this paper is as follows. The explicit solutions to closure equations of the general plane-symmetric Bricard linkage are derived and the comparison between kinematics variations of different plane-symmetric Bricard linkages based on these solutions are discussed in section 2. Section 3 introduces the derived  $5R/4R$  linkages from the general case and their corresponding geometric conditions. Section 4 addresses the bifurcation between the plane-symmetric Bricard linkage and the Bennett linkage. Section 5 discusses other various bifurcation cases of the plane-symmetric Bricard linkage under different geometric conditions. Final conclusions are drawn in section 6.

## 2. The explicit solutions to closure equations and kinematic properties of the general plane-symmetric Bricard linkage

The geometrical parameters of the general plane-symmetric Bricard linkage are shown in Fig. 1 with the conditions that

$$a_{12} = a_{61} = a, \quad a_{23} = a_{56} = b, \quad a_{34} = a_{45} = c,$$

$$\alpha_{12} = 2\pi - \alpha_{61} = \alpha, \quad \alpha_{23} = 2\pi - \alpha_{56} = \beta, \quad \alpha_{34} = 2\pi - \alpha_{45} = \gamma, \quad (1)$$

$$R_1 = R_4 = 0, \quad R_6 = -R_2, \quad R_5 = -R_3.$$

The setup of coordinate frames is in accordance with the Denavit and Hartenberg's convention [17], where  $z_i$  is along the revolute axis of joint  $i$ ;  $x_i$  is the common normal direction pointing from  $z_{i-1}$  to  $z_i$ ;  $a_{i(i+1)}$  is the normal distance between  $z_i$  and  $z_{i+1}$  (also known as the length of link  $i(i+1)$ );  $\alpha_{i(i+1)}$  is the angle of rotation from  $z_i$  to  $z_{i+1}$  about axis  $x_i$  (also known as the twist of link  $i(i+1)$ );  $R_i$  is the normal distance between  $x_i$  and  $x_{i+1}$  (also known as the offset of joint  $i$ ); and  $\theta_i$  is the angle of rotation from  $x_i$  and  $x_{i+1}$  about axis  $z_i$  (also known as the kinematic variable of joint  $i$ ). Here,  $a$ ,  $b$ ,  $c$ ,  $\alpha$ ,  $\beta$ ,  $\gamma$ ,  $R_2$  and  $R_3$  are taken as the geometrical parameters of the plane-symmetric Bricard linkage.

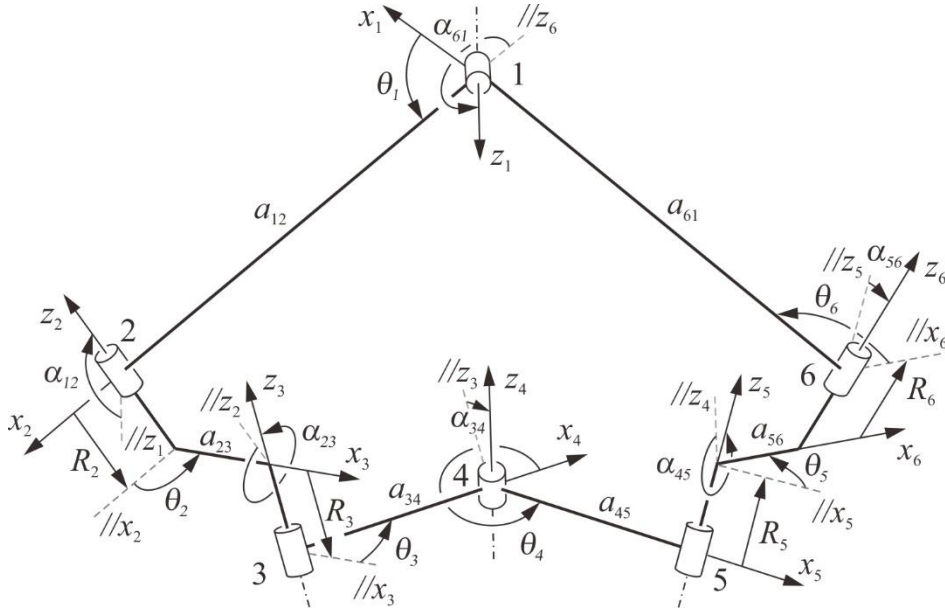


Fig. 1 D-H parameters of the plane-symmetric Bricard linkage

As it is a single loop linkage, the closure equation of the general plane-symmetric Bricard linkage can be written as

$$\mathbf{T}_{21} \cdot \mathbf{T}_{32} \cdot \mathbf{T}_{43} = \mathbf{T}_{61} \cdot \mathbf{T}_{56} \cdot \mathbf{T}_{45}, \quad (2)$$

where the transformation matrix  $\mathbf{T}_{(i+1)i}$  is

$$\mathbf{T}_{(i+1)i} = \begin{bmatrix} \cos \theta_i & -\cos \alpha_{i(i+1)} \sin \theta_i & \sin \alpha_{i(i+1)} \sin \theta_i & a_{i(i+1)} \cos \theta_i \\ \sin \theta_i & \cos \alpha_{i(i+1)} \cos \theta_i & -\sin \alpha_{i(i+1)} \cos \theta_i & a_{i(i+1)} \sin \theta_i \\ 0 & \sin \alpha_{i(i+1)} & \cos \alpha_{i(i+1)} & R_i \\ 0 & 0 & 0 & 1 \end{bmatrix}, \quad (3)$$

which transforms the expression in the  $i+1$ th coordinate system to the  $i$ th coordinate system, and  $\mathbf{T}_{i(i+1)} = \mathbf{T}_{(i+1)i}^{-1}$ .

Due to the plane symmetry, we have

$$\theta_5 = \theta_3, \quad \theta_6 = \theta_2. \quad (4)$$

Substituting Eq. (4) to Eq. (2) and simplifying entries (1, 3) and (1, 4) in Eq. (2) (shown in **Appendix A**), the following equation is obtained

$$\begin{aligned} & \frac{\sin \gamma (\cos \theta_2 \sin \theta_3 + \cos \beta \sin \theta_2 \cos \theta_3) + \sin \beta \cos \gamma \sin \theta_2}{\left( \cos \alpha \sin \gamma \sin \theta_2 \sin \theta_3 - \cos \alpha \cos \beta \sin \gamma \cos \theta_2 \cos \theta_3 \right.} \\ & \left. + \sin \alpha \sin \beta \sin \gamma \cos \theta_3 - \cos \alpha \sin \beta \cos \gamma \cos \theta_2 - \sin \alpha \cos \beta \cos \gamma \right)} \\ & = \frac{c(\cos \theta_2 \cos \theta_3 - \cos \beta \sin \theta_2 \sin \theta_3) + b \cos \theta_2 + a + R_3 \sin \beta \sin \theta_2}{\left[ c(\cos \alpha \sin \theta_2 \cos \theta_3 + \cos \alpha \cos \beta \cos \theta_2 \sin \theta_3 - \sin \alpha \sin \beta \sin \theta_3) \right.} \\ & \left. + b \cos \alpha \sin \theta_2 - R_3 \cos \alpha \sin \beta \cos \theta_2 - R_2 \sin \alpha - R_3 \sin \alpha \cos \beta \right]} \end{aligned} \quad (5)$$

which can be further simplified as

$$A \tan^2 \frac{\theta_3}{2} + B \tan \frac{\theta_3}{2} + C = 0, \quad (6)$$

where  $\theta_2$  is taken as the input kinematic variable, and

$$\begin{aligned} A &= (a - b + c) \sin(\alpha - \beta + \gamma) \tan^2 \frac{\theta_2}{2} + 2 \sin \alpha (R_3 \sin \gamma + R_2 \sin(\gamma - \beta)) \tan \frac{\theta_2}{2}, \\ &+ (a + b - c) \sin(\alpha + \beta - \gamma) \end{aligned}$$

$$\begin{aligned} B &= 2 \sin \gamma (R_2 \sin \alpha + R_3 \sin(\alpha - \beta)) \tan^2 \frac{\theta_2}{2} + 2((a - c) \sin(\alpha - \gamma) - (a + c) \sin(\alpha + \gamma)) \tan \frac{\theta_2}{2}, \\ &- 2 \sin \gamma (R_2 \sin \alpha + R_3 \sin(\alpha + \beta)) \end{aligned}$$

$$C = (a-b-c)\sin(\alpha-\beta-\gamma)\tan^2\frac{\theta_2}{2} + 2\sin\alpha(R_3\sin\gamma + R_2\sin(\gamma+\beta))\tan\frac{\theta_2}{2} \\ + (a+b+c)\sin(\alpha+\beta+\gamma)$$

Moreover, the other kinematic variables  $\theta_1$  and  $\theta_4$  could be calculated by simplifying entries (1, 3) and (3, 1) in Eq. (2) (shown in **Appendix A**) as

$$\tan\frac{\theta_1}{2} = \frac{\sin\gamma(\cos\theta_2\sin\theta_3 + \cos\beta\sin\theta_2\cos\theta_3) + \sin\beta\cos\gamma\sin\theta_2}{\left(\cos\alpha\sin\gamma\sin\theta_2\sin\theta_3 - \cos\alpha\cos\beta\sin\gamma\cos\theta_2\cos\theta_3 \right. \\ \left. + \sin\alpha\sin\beta\sin\gamma\cos\theta_3 - \cos\alpha\sin\beta\cos\gamma\cos\theta_2 - \sin\alpha\cos\beta\cos\gamma\right)}, \quad (7)$$

$$\tan\frac{\theta_4}{2} = \frac{\sin\alpha\sin\theta_2\cos\theta_3 + \sin\theta_3(\sin\alpha\cos\beta\cos\theta_2 + \cos\alpha\sin\beta)}{\left[\cos\gamma(\sin\alpha\sin\theta_2\sin\theta_3 - \sin\alpha\cos\beta\cos\theta_2\cos\theta_3 - \cos\alpha\sin\beta\cos\theta_3) \right. \\ \left. + \sin\gamma(\sin\alpha\sin\beta\cos\theta_2 - \cos\alpha\cos\beta)\right]}. \quad (8)$$

The solutions to Eq. (6) can be divided into following three cases.

1) When  $A=0$ ,

$$\tan\frac{\theta_3}{2} = \frac{-C}{B}. \quad (9)$$

Substituting Eq. (9) to Eqs. (7) and (8), the relationship between  $\theta_1$ ,  $\theta_4$  and  $\theta_2$  can be derived as

$$\tan\frac{\theta_1}{2} = \frac{D}{E}, \quad (10)$$

$$\tan\frac{\theta_4}{2} = \frac{F}{G}, \quad (11)$$

in which the terms  $D$ - $G$  are listed in the **Appendix B**.

Therefore, Eqs. (4), (9), (10) and (11) form the only set of explicit solutions to closure equation of the plane-symmetric Bricard linkage when  $A=0$ . According to the definition of term  $A$ , the following equation can be obtained

$$\left( (a-b+c)\sin(\alpha-\beta+\gamma)\tan^2\frac{\theta_2}{2} + 2\sin\alpha(R_3\sin\gamma + R_2\sin(\gamma-\beta))\tan\frac{\theta_2}{2} \right. \\ \left. + (a+b-c)\sin(\alpha+\beta-\gamma) \right) = 0 \quad (12)$$

Eq. (12) should be always true for all values of  $\theta_2$ , so we have

$$\begin{cases} (a-b+c)\sin(\alpha-\beta+\gamma)=0 \\ 2\sin\alpha(R_3\sin\gamma+R_2\sin(\gamma-\beta))=0. \\ (a+b-c)\sin(\alpha+\beta-\gamma)=0 \end{cases} \quad (13)$$

Therefore, the geometric conditions for a plane-symmetric Bricard linkage with only one solution in this case are

$$\begin{cases} a-b+c=0 \text{ or } \alpha-\beta+\gamma=k_1\pi \\ \alpha=k_2\pi \text{ or } R_3\sin\gamma+R_2\sin(\gamma-\beta)=0, \\ a+b-c=0 \text{ or } \alpha+\beta-\gamma=k_3\pi \end{cases} \quad (14)$$

where  $k_1, k_2, k_3 \in R$ .

2) When  $A \neq 0$  and  $\Delta = B^2 - 4AC \geq 0$ , the relationship between  $\theta_3$  and  $\theta_2$  are

$$\tan \frac{\theta_3}{2} = \frac{-B \pm \sqrt{B^2 - 4AC}}{2A}. \quad (15)$$

Further, substituting Eq. (15) to Eqs. (7) and (8), we have

$$\tan \frac{\theta_1}{2} = \frac{HI + J}{KI + L}, \quad (16)$$

$$\tan \frac{\theta_4}{2} = \frac{MI + N}{OI + P}, \quad (17)$$

in which the terms  $H-P$  are listed in the **Appendix B**.

Therefore, when  $A \neq 0$  and  $\Delta \geq 0$ , the solutions to closure equation of the plane-symmetric Bricard linkage are the equation set (4), (15), (16) and (17). Applying the definition of the terms  $A$ ,  $B$  and  $C$  to the discriminant  $\Delta$ , a quartic equation with


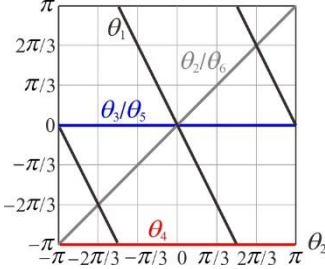
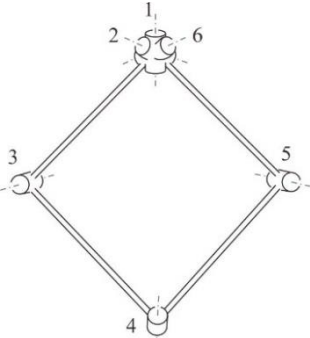
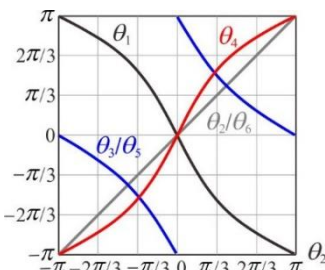
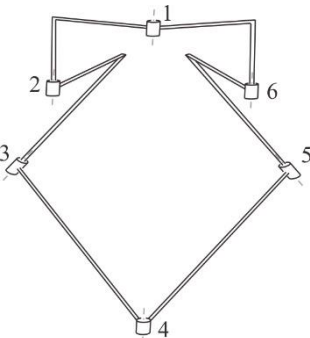
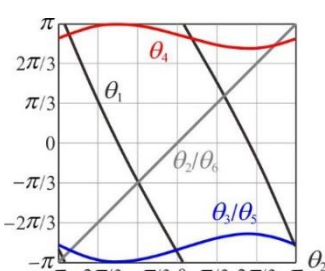
$\tan \frac{\theta_2}{2}$  being the independent variable can be obtained. According to the

characteristics of the curve of quartic equation, the discriminant is semi-positive only under the conditions that the highest-degree coefficient and the minimum value of the discriminant  $\Delta$  are non-negative.

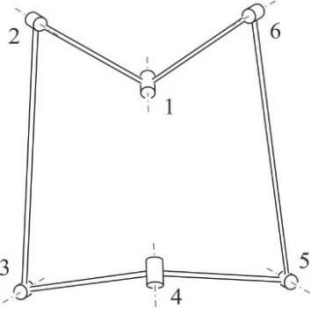
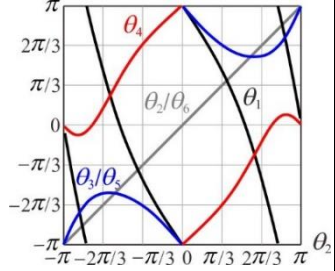
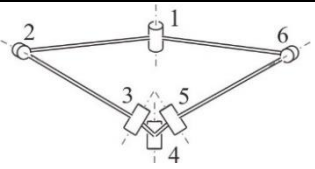
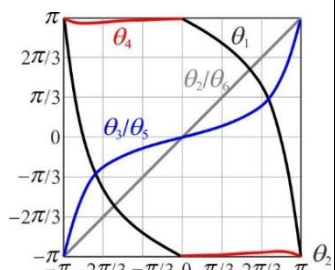
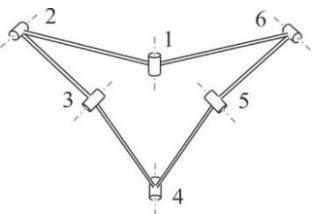
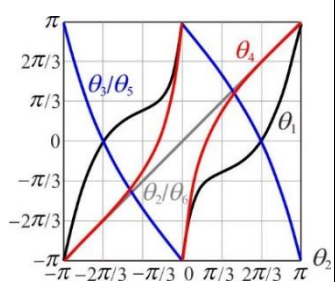
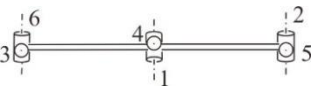
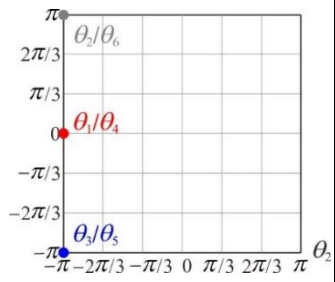
3) When  $A \neq 0$  and  $\Delta < 0$ , there is no solution to Eq. (6), which means that the linkage is a rigid structure.

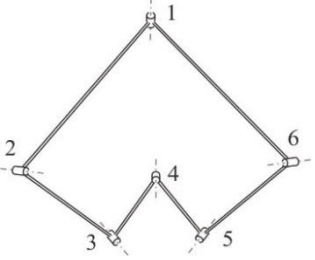
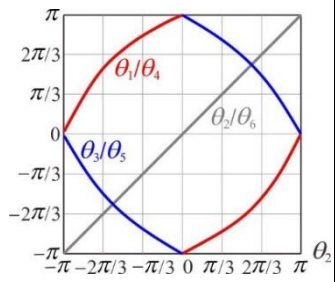
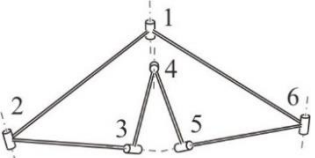
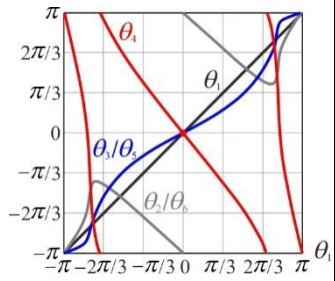
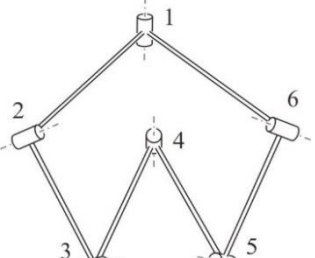
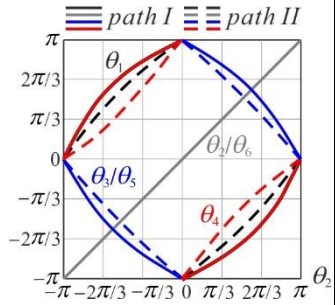
Based on explicit solutions, the plane-symmetric Bricard linkage can be classified by the values of  $A$  and  $\Delta$ . The detailed kinematic paths and motion behaviour of the plane-symmetric Bricard linkage with different geometric conditions are given in Table 1.

Table 1. The kinematic properties of the plane-symmetric Bricard linkage

Case	Geometric condition	Linkage model	Kinematic paths		
			N	curves	Motion behaviour
1	$A = 0,$ $a = 0, b = c,$ $\alpha = k_2\pi.$	 <p>Geometrical parameters:  <math>a = 0, b = c = 1,</math>  <math>\alpha = 0, \beta = \pi/3, \gamma = \pi/6,</math>  <math>R_2 = R_3 = 0.</math></p>	1		Three joint axes 6, 1 and 2 coincide and the linkage would rotate along this joint as a whole. $\theta_2 = \theta_6$ , while $\theta_1 = -2\theta_2$ .
2	$A = 0,$ $a = 0, b = c,$ $R_2 \sin(\gamma - \beta) = -R_3 \sin \gamma.$	 <p>Geometrical parameters:  <math>a = 0, b = c = 1,</math>  <math>\alpha = \frac{\pi}{3}, \beta = \gamma = \frac{\pi}{6},</math>  <math>R_2 = R_3 = 0.</math></p>	1		The linkage has a 6R motion branch with joint axes 6, 1 and 2 intersect.
3	$A = 0,$ $\alpha = k_2\pi,$ $\beta - \gamma = (k_2 - k_1)\pi.$	 <p>Geometrical parameters:</p>	1		The linkage has a 6R motion branch with joint axes 6, 1 and 2 parallel.



		$a = 1, b = 2, c = 4,$ $\alpha = 0, \beta = 7\pi / 6, \gamma = \pi / 6,$ $R_2 = -1, R_3 = -2.$			
4	$A = 0,$ $b = a + c,$ $\alpha + \beta - \gamma$ $= k_3\pi,$ $R_2 \sin(\gamma - \beta)$ $= -R_3 \sin \gamma.$	 <p>Geometrical parameters:  <math>a = c = 1, b = 2,</math>  <math>\alpha = \beta = \pi / 6, \gamma = \pi / 3,</math>  <math>R_2 = R_3 = 0.</math></p>	1		The linkage has a 6R motion branch.
5	$A = 0,$ $c = a + b,$ $\alpha - \beta + \gamma$ $= k_1\pi,$ $R_2 \sin(\gamma - \beta)$ $= -R_3 \sin \gamma.$	 <p>Geometrical parameters:  <math>a = b = 1, c = 2,</math>  <math>\alpha = \pi / 3, \beta = \pi / 2, \gamma = \pi / 6,</math>  <math>R_2 = R_3 = 0.</math></p>	1		The linkage has a 6R motion branch.
6	$A = 0,$ $\alpha = \frac{(k_1 + k_3)\pi}{2},$ $\beta - \gamma$ $= \frac{(k_3 - k_1)\pi}{2},$ $R_2 \sin(\gamma - \beta)$ $= -R_3 \sin \gamma.$	 <p>Geometrical parameters:  <math>a = 1.5, b = 1, c = 2,</math>  <math>\alpha = \frac{\pi}{2}, \beta = \frac{\pi}{4}, \gamma = -\frac{\pi}{4},</math>  <math>R_2 = R_3 = 0.</math></p>	1		The linkage has a 6R motion branch.
7	$A \neq 0,$ $\Delta < 0.$	 <p>Geometrical parameters:  <math>a = c = 1, b = 2,</math>  <math>\alpha = \gamma = \frac{\pi}{6}, \beta = \frac{\pi}{2},</math>  <math>R_2 = R_3 = 0.</math></p>	0		The mechanism is a rigid structure and no motion exists.

8	$A \neq 0, \Delta = 0.$	 <p>Geometrical parameters:  <math>a = 3, b = 2, c = 1,</math>  <math>\alpha = \frac{2\pi}{3}, \beta = \frac{\pi}{6}, \gamma = -\frac{\pi}{6},</math>  <math>R_2 = R_3 = 0.</math></p>	1		The linkage has only one 6R motion branch.
9	$A \neq 0, \Delta > 0.$	 <p>Geometrical parameters:  <math>a = 3, b = 2, c = 1,</math>  <math>\alpha = \frac{\pi}{12}, \beta = \frac{\pi}{3}, \gamma = \frac{\pi}{4},</math>  <math>R_2 = R_3 = 0.</math></p>	1		Because joints 2 and 6 have no complete rotation. (So joint 1 is taken as input in left figure.) Joint 4 rotates three angular strokes while joints 1, 3 and 5 rotate one.
10	$A \neq 0, \Delta > 0.$	 <p>Geometrical parameters:  <math>a = 2, b = c = 1,</math>  <math>\alpha = \frac{2\pi}{3}, \beta = \frac{\pi}{6}, \gamma = -\frac{\pi}{6},</math>  <math>R_2 = R_3 = 0.</math></p>	2		The linkage has two different plane-symmetric 6R motion branches corresponding to two kinematic paths, shown in the kinematic curves as solid and dash lines, respectively.

Several typical cases can be seen from Table 1 as follows.

- (1) When  $A = 0$ , six cases (Cases 1 to 6) can be derived from Eq. (14) where only one kinematic path exists.
- (2) When  $A \neq 0$  and  $\Delta < 0$ , there is no kinematic path, i.e., the mechanism is rigid structure in Case 7.
- (3) When  $A \neq 0$  and  $\Delta = 0$ , there is one kinematic path, corresponding to Case 8.
- (4) When  $A \neq 0$  and  $\Delta > 0$ , there are two set of solutions with  $\theta_2$  as the input variable. A careful check reveals that for Case 10, two sets of different kinematic curves exists corresponding to two different linkage closures, which can switch to

each other at the collinear configurations.

However, there is an exception as Case 9. When  $A \neq 0, \Delta > 0$ , taking  $\theta_2$  as the input variable, there are two sets of solutions. Yet, if converting them into the format with  $\theta_1$  as the input variable, there is only one set of explicit solutions, i.e., one kinematic path obtained. This is because that the  $\theta_2$  has no complete rotation in the whole path.

### 3. Derived 5R/4R linkages from the general plane-symmetric Bricard linkage

The above solutions to the closure equations of the general plane-symmetric Bricard linkage are conditional to the constraint that  $\theta_i \neq \pi$  ( $i = 1, 2, 3, 4, 5, 6$ ). When any one of the kinematic variable  $\theta_i$  is kept to  $\pi$ , the linkage may degenerate to 5R/4R linkages.

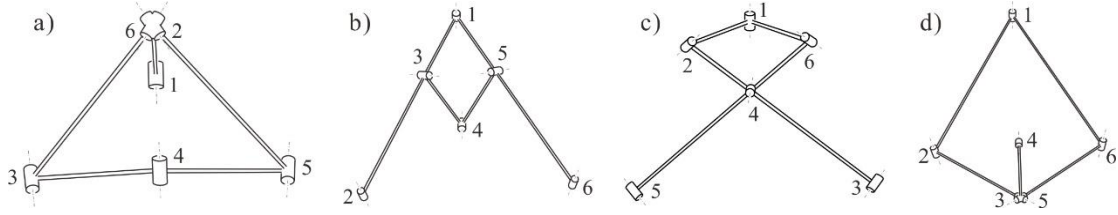


Fig. 2 The degenerated plane-symmetric Bricard linkage: a) when  $\theta_1 = \pi$ ; b) when  $\theta_2 = \theta_6 = \pi$ ; c) when  $\theta_3 = \theta_5 = \pi$ ; d) when  $\theta_4 = \pi$ .

#### 1) When $\theta_1 = \pi$

As shown in Fig. 2a), link 12 coincides with link 61 in this case, making the resultant linkage a 5R linkage. The problem is to find out when the linkage is moveable.

Substituting  $\theta_1 = \pi$  to the closure equation Eq. (2), it is found that the linkage is moveable only when entries (2,3) and (2,4) of Eq. (2) (shown in **Appendix A**), which contain kinematic variables  $\theta_2$  and  $\theta_3$ , are linearly dependent. Thus, the geometric condition to make the plane-symmetric Bricard linkage degenerate to a movable 5R linkage can be derived from

$$\begin{aligned}
& \begin{bmatrix} \sin(\beta - \alpha - \gamma)m^2 + \sin(\gamma - \alpha - \beta) \\ 4\cos\alpha\sin\gamma m \\ \sin(\alpha - \beta - \gamma)m^2 - \sin(\alpha + \beta + \gamma) \end{bmatrix}^T \begin{bmatrix} n^2 \\ n \\ 1 \end{bmatrix} \\
& = k \begin{bmatrix} [R_3\sin(\beta - \alpha) - R_2\sin\alpha]m^2 + 2(b - c)\cos\alpha m - R_3\sin(\alpha + \beta) - R_2\sin\alpha \\ -2c\cos(\alpha - \beta)m^2 + 2c\cos(\alpha + \beta) \\ [R_3\sin(\beta - \alpha) - R_2\sin\alpha]m^2 + 2(b + c)\cos\alpha m - R_3\sin(\alpha + \beta) - R_2\sin\alpha \end{bmatrix}^T \begin{bmatrix} n^2 \\ n \\ 1 \end{bmatrix}, \quad (18)
\end{aligned}$$

where  $m = \tan \frac{\theta_2}{2}$ ,  $n = \tan \frac{\theta_3}{2}$  and  $k \in R$ .

The type of the degenerated linkage is depending on the choice of geometrical parameters that meet Eq. (18). The plane-symmetric Bricard linkage could degenerate to a planar 5R linkage as shown in Fig. 3a) when all twist is zero whatever the values of link lengths and offsets are. In this case, the joint 1 is disabled since  $\theta_1$  is kept to  $\pi$ . The resultant planar 5R linkage has two joints 2 and 6 coincide, which works as two separated parts including a rotation motion about joint 2/6 and a planar 4R motion formed by joints 3, 4, 5 and 2/6.

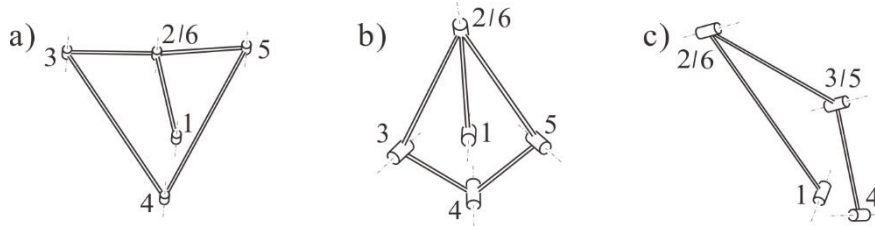


Fig. 3 The plane-symmetric Bricard when  $\theta_1 = \pi$  : a) the degenerated planar 5R linkage with two joints 2 and 6 coincide; b) the degenerated spherical 5R linkage with two joints 2 and 6 coincide; c) the degenerated serial kinematic chain with joints 2, 6 and 3, 5 both coincide.

As shown in Fig. 3b), the plane-symmetric Bricard linkage could also degenerate to a spherical 5R linkage if we set all link lengths and offsets zero. Take

$a = b = c = 0$ ,  $\alpha = \frac{\pi}{4}$ ,  $\beta = \frac{\pi}{3}$ ,  $\gamma = \frac{\pi}{5}$ ,  $R_2 = R_3 = 0$  as an example. The resultant spherical

5R linkage also has two joints 2 and 6 coincide, so the resultant linkage works as a spherical 4R linkage formed by joints 3, 4, 5 and 2/6 with an additional rotation about joint 2/6.

Besides, the plane-symmetric Bricard linkage would degenerate to an equivalent serial kinematic chain with revolute joints when the parameters are set

$a = b = 1, c = 1, \alpha = \frac{\pi}{2}, \beta = 0, \gamma = \frac{\pi}{2}, R_2 = R_3 = 0$  as shown in Fig. 3c). In this case,

joints 2, 6 and 3, 5 coincide. The resultant linkage works as a serial kinematic chain with two effective revolute joints 2/6 and 3/5.

2) When  $\theta_2 = \theta_6 = \pi$

As shown in Fig. 2b), links 12 and 23 are coincident as well as links 56 and 61, which generate a 4R linkage. In order to make the linkage moveable, we need to substitute

$\theta_2 = \theta_6 = \pi$  to the closure equation as Eq. (2). Taking entries (1,3) and (1,4) of Eq. (2)

(shown in **Appendix A**), which contain kinematic variables  $\theta_1$  and  $\theta_3$ , the linkage is moveable only when the following equation is satisfied

$$\frac{-\sin \gamma \sin \theta_3}{\sin \gamma \cos(\alpha - \beta) \cos \theta_3 + \cos \gamma \sin(\beta - \alpha)} = \frac{-c \cos \theta_3 - b + a}{-c \cos(\alpha - \beta) \sin \theta_3 + R_3 \sin(\beta - \alpha) - R_2 \sin \alpha}. \quad (19)$$

Further, to make Eq. (19) always true for all values of  $\theta_3$ , the geometric condition to make the plane-symmetric Bricard linkage degenerate to a movable 4R linkage is

$$b - a + c = 0, c \sin(\gamma + \alpha - \beta) = 0, \sin \gamma [R_2 \sin \alpha - R_3 \sin(\beta - \alpha)] = 0, \quad (20)$$

or

$$\sin(\beta - \alpha + \gamma) = 0, (a - b + c) \sin 2\gamma = 0, \sin \gamma [R_2 \sin \alpha - R_3 \sin(\beta - \alpha)] = 0. \quad (21)$$

The type of the resultant 4R linkage depends on the choice of geometrical parameters that meet Eq. (20) or (21). For example, if we set the geometric condition as

$a = b = c = 0, R_2 = R_3 = 0$ , the movable linkage is a spherical 4R linkage. If the

condition is  $\alpha = \beta = \gamma = 0, R_2 = R_3 = 0$ , the linkage degenerates to a planar 4R

linkage. Moreover, a Bennett linkage is obtained when the condition is set as

$a = b + c, \beta = \alpha + \gamma, R_2 = R_3 = 0$  or  $b = a + c, \alpha = \beta + \gamma, R_2 = R_3 = 0$ .

3) When  $\theta_3 = \theta_5 = \pi$

Similarly, in Fig. 2c) links 23 and 34 are coincident as well as links 45 and 56, which makes the linkage generates a 4R linkage. The condition of a moveable 4R linkage is

obtained by substituting  $\theta_3 = \theta_5 = \pi$  to the closure equation Eq. (2). Considering entries

(1,3) and (1,4) of Eq. (2) (shown in **Appendix A**), which contain kinematic variables  $\theta_1$  and  $\theta_2$ , the linkage is moveable only when

$$\begin{aligned} & \frac{\sin(\beta - \gamma) \sin \theta_2}{\cos \alpha \sin(\gamma - \beta) \cos \theta_2 - \sin \alpha \cos(\beta - \gamma)} \\ &= \frac{(b - c) \cos \theta_2 + R_3 \sin \beta \sin \theta_2 + a}{(b - c) \cos \alpha \sin \theta_2 - R_3 \cos \alpha \sin \beta \cos \theta_2 - R_3 \sin \alpha \cos \beta - R_2 \sin \alpha} \end{aligned} \quad , \quad (22)$$

i.e.,

$$a - b + c = 0, a \sin(\gamma - \alpha - \beta) = 0, \sin \alpha [R_2 \sin(\beta - \gamma) - R_3 \sin \gamma] = 0, \quad (23)$$

or

$$\sin(\alpha - \beta + \gamma) = 0, (a + b - c) \sin 2\alpha = 0, \sin \alpha [R_2 \sin(\beta - \gamma) - R_3 \sin \gamma] = 0. \quad (24)$$

The type of the resultant movable 4R linkage varies with the choice of geometrical parameters according to Eq. (23) or (24). When all link lengths and offsets are set zeros, the resultant 4R linkage could be a spherical 4R linkage. When all twists and offsets are zeros, a planar 4R linkage is obtained. The condition to obtain a Bennett linkage is  $b = a + c, \gamma = \alpha + \beta, R_2 = R_3 = 0$  or  $c = a + b, \beta = \alpha + \gamma, R_2 = R_3 = 0$ .

4) When  $\theta_4 = \pi$

As shown in Fig. 2d), link 34 coincides with link 45 in this case, making the resultant linkage a 5R linkage. Substituting  $\theta_4 = \pi$  to the closure equation Eq. (2), it is found that the linkage is moveable only when entries (1,3), (1,4) and (3,2) of Eq. (2) (shown in **Appendix A**), which contain kinematic variable  $\theta_1$ ,  $\theta_2$  and  $\theta_3$ , are linearly dependent. Thus, the geometric condition to make the plane-symmetric Bricard linkage degenerate to a movable 5R linkage the following equation can be derived as

$$\begin{aligned}
& \begin{bmatrix} \left( (a-b+c)\sin(\alpha-\beta+\gamma)m^2 + 2\sin\alpha(R_3\sin\gamma + R_2\sin(\gamma-\beta))m \right) \\ + (a+b-c)\sin(\alpha+\beta-\gamma) \\ \left( 2\sin\gamma(R_2\sin\alpha + R_3\sin(\alpha-\beta))m^2 + 2((a-c)\sin(\alpha-\gamma)) \right) \\ - (a+c)\sin(\alpha+\gamma)m - 2\sin\gamma(R_2\sin\alpha + R_3\sin(\alpha+\beta)) \\ \left( (a-b-c)\sin(\alpha-\beta-\gamma)m^2 + 2\sin\alpha(R_3\sin\gamma + R_2\sin(\gamma+\beta))m \right) \\ + (a+b+c)\sin(\alpha+\beta+\gamma) \end{bmatrix}^T \begin{bmatrix} n^2 \\ n \\ 1 \end{bmatrix}, \quad (25) \\
& = k \begin{bmatrix} \sin(\beta-\alpha-\gamma)m^2 + \sin(\alpha+\beta-\gamma) \\ 4\sin\alpha\sin\gamma m \\ \sin(\alpha-\beta-\gamma)m^2 - \sin(\alpha+\beta+\gamma) \end{bmatrix}^T \begin{bmatrix} n^2 \\ n \\ 1 \end{bmatrix}
\end{aligned}$$

where  $m = \tan \frac{\theta_2}{2}$ ,  $n = \tan \frac{\theta_3}{2}$  and  $k \in R$ . Considering the plane symmetry of the

Bricard linkage, the degenerated linkage is similar as the case when  $\theta_1 = \pi$ .

Moreover, when  $\theta_i$  is kept constant but not equal to  $\pi$ , the linkage will also degenerate to  $5R/4R$  linkages.

#### 4. Bifurcation between the plane-symmetric Bricard linkage and the Bennett linkage

Based on the analysis in section 3, in cases 2 and 3, the linkage could bifurcate from the plane-symmetric Bricard linkage to the Bennett linkage. When the geometric condition is

$$a = b + c, \beta = \alpha + \gamma, R_2 = R_3 = 0 \text{ or } b = a + c, \alpha = \beta + \gamma, R_2 = R_3 = 0, \quad (26)$$

$A \neq 0$  and  $\Delta > 0$ . The linkage would have two solutions given as the equation set (4), (15), (16) and (17). However, there is only one plane-symmetric  $6R$  motion branch represented by the solid line shown in Fig. 4, which corresponds to Case 9 in Table 1.

The revolute joints  $\theta_2$  and  $\theta_6$  have no complete rotation.

Moreover, there is another motion branch when  $\theta_2 = \theta_6 = \pi$ , shown as the dashed line in Fig. 4, where the linkage works as a Bennett linkage actually. The whole bifurcation process is presented in Fig. 4, where the actuated joint 1 is highlighted with a rotation in red.

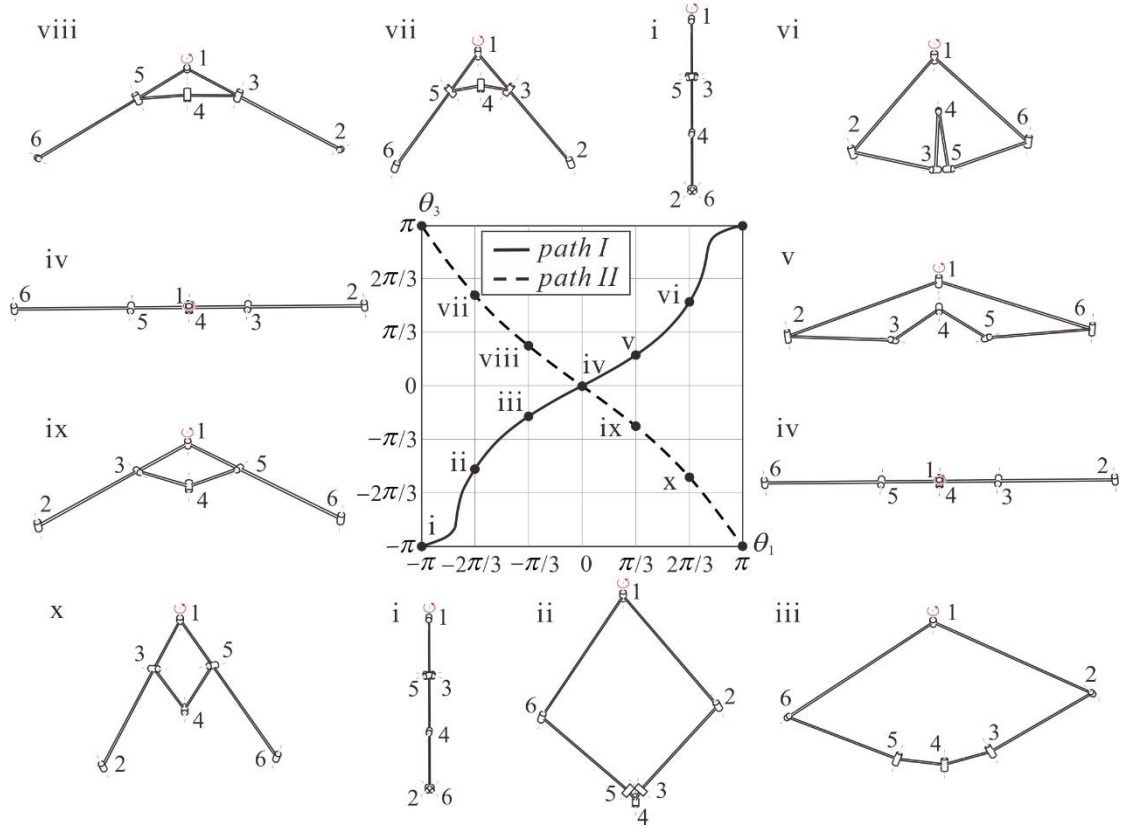


Fig. 4 Bifurcation between the plane-symmetric Bricard linkage and the Bennett linkage when  $\theta_2 = \theta_6 = \pi$ , where i-ii-iii-iv-v-vi-i correspond to configurations of the linkage along the plane-symmetric Bricard motion branch and i-vii-viii-vi-ix-x-i correspond to configurations of the linkage along the Bennett motion branch. Here the geometrical parameters of this linkage are  $a = 3, b = 2, c = 1, \alpha = \frac{\pi}{12}, \beta = \frac{\pi}{3}, \gamma = \frac{\pi}{4}, R_2 = R_3 = 0$ .

Similarly, once the geometric conditions are

$$b = a + c, \gamma = \alpha + \beta, R_2 = R_3 = 0 \quad \text{or} \quad c = a + b, \beta = \alpha + \gamma, R_2 = R_3 = 0, \quad (27)$$

$A = 0$ . The linkage would have only one  $6R$  motion branch given as the equation set (4), (9), (10) and (11), which is represented by the solid line shown in Fig. 5 where the actuated joint 2 is highlighted with a rotation in red.

All the revolute joints have complete rotation, and some revolute joints have strokes more than  $2\pi$  such as the stroke of  $\theta_1$  is  $6\pi$ . And there is one more motion branch when  $\theta_3 = \theta_5 = \pi$ , as the dashed line in Fig. 5, in which the linkage also works as a Bennett linkage.



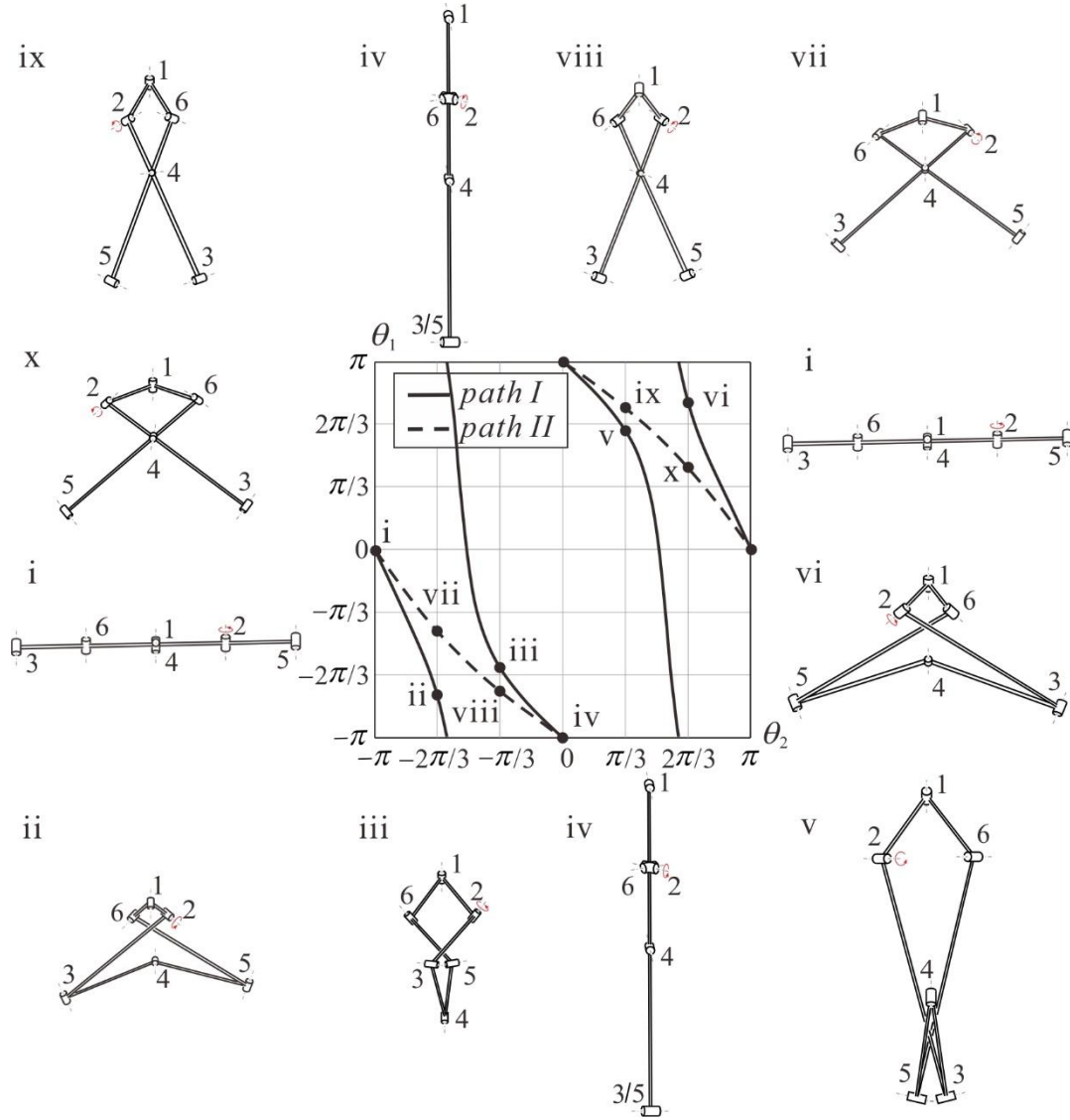


Fig. 5 Bifurcation between the plane-symmetric Bricard linkage and the Bennett linkage when  $\theta_3 = \theta_5 = \pi$ , where i-ii-iii-iv-v-vi-i correspond to configurations of the linkage along the plane-symmetric Bricard motion branch and i-vii-viii-vi-ix-x-i correspond to configurations of the linkage along the Bennett motion branch. Here the geometrical parameters of this linkage are  $a = 1, b = 3, c = 2, \alpha = \frac{\pi}{4}, \beta = \frac{\pi}{3}, \gamma = \frac{7\pi}{12}, R_2 = R_3 = 0$ .

## 5. Other bifurcation behaviours of the plane-symmetric Bricard linkage

The last section deals with a special case of the bifurcation between the plane-symmetric Bricard linkage and the Bennett linkage. Additional various bifurcation cases depending on the different choice of geometrical parameters are revealed in this section.

### 1) Bifurcation between two plane-symmetric Bricard linkage motion branches

In order to make the plane-symmetric Bricard linkage have two  $6R$  motion branches,  $A \neq 0$  and  $\Delta > 0$  must be satisfied according to the analysis in section 2. If we set the geometric condition as

$$a = 2d, b = d, c = d, \alpha = \pi - 2\delta, \beta = \delta, \gamma = -\delta, R_2 = R_3 = 0, \quad (28)$$

the linkage would have two solutions as

$$\tan \frac{\theta_2}{2} = -\frac{1}{\cos 2\delta} / \tan \frac{\theta_1}{2}, \quad \tan \frac{\theta_3}{2} = -\cos \delta \tan \frac{\theta_1}{2}, \quad \theta_4 = \theta_1, \quad \theta_5 = \theta_3, \quad \theta_6 = \theta_2. \quad (29)$$

and

$$\begin{aligned} \tan \frac{\theta_1}{2} &= -\frac{1}{\cos^2 \delta} / \tan \frac{\theta_6}{2}, \quad \tan \frac{\theta_3}{2} = \frac{1}{\cos \delta} / \tan \frac{\theta_6}{2}, \\ \tan \frac{\theta_4}{2} &= -\frac{\cos 2\delta \tan^2 \frac{\theta_6}{2} + 1}{\tan \frac{\theta_6}{2} (\cos^2 \delta \tan^2 \frac{\theta_2}{2} + 2 - \cos^2 \delta)}, \quad \theta_2 = \theta_6, \quad \theta_5 = \theta_3. \end{aligned} \quad (30)$$

As shown in Fig. 6, the two kinematic paths intersect at points  $(\pi, 0)$  and  $(0, \pi)$ , indicating these two points are the bifurcation points. The actuated joint is highlighted with a rotation in red. The linkage would work along *path I* if we choose joint 1 as the actuated joint, and it would change to *path II* when the actuated joint is joint 2.

## 2) Bifurcation among equivalent kinematic chains with revolute joints and a four-bar double-rocker linkage

There is a special case where  $A$ ,  $B$  and  $C$  all equal to zero, where the solution set in section 2 is no longer true. For example, if we set the geometrical parameters as

$$a = 3, b = 2, c = 4, \alpha = \frac{\pi}{2}, \beta = 0, \gamma = \frac{\pi}{2}, R_2 = R_3 = 0, \quad (31)$$

by solving Eq. (2), the solutions can be obtained as

$$\theta_1 = -\theta_4, \theta_2 = \theta_6 = \frac{\pi}{3}, \theta_3 = \theta_5 = \frac{2\pi}{3}, \quad (32a)$$

$$\theta_1 = -\theta_4, \theta_2 = \theta_6 = -\frac{\pi}{3}, \theta_3 = \theta_5 = -\frac{2\pi}{3}, \quad (32b)$$

$$\theta_1 = \theta_4 = \pi, \theta_2 = \theta_6 \in (-\pi, \pi), \theta_3 = \theta_5 \in (-\pi, \pi), \quad (32c)$$

and

$$\theta_1 = \theta_4 = 0, \tan \frac{\theta_6}{2} = \frac{-4 \tan \frac{\theta_2}{2} \pm \sqrt{3(7 \tan^2 \frac{\theta_2}{2} + 3)(7 - 5 \tan^2 \frac{\theta_2}{2})}}{15 \tan^2 \frac{\theta_2}{2} + 7}, \quad (32d)$$

$$\sin(\theta_2 + \theta_3) = \frac{\sin \theta_6 - \sin \theta_2}{4}, \theta_5 = -(\theta_2 + \theta_3 + \theta_6).$$

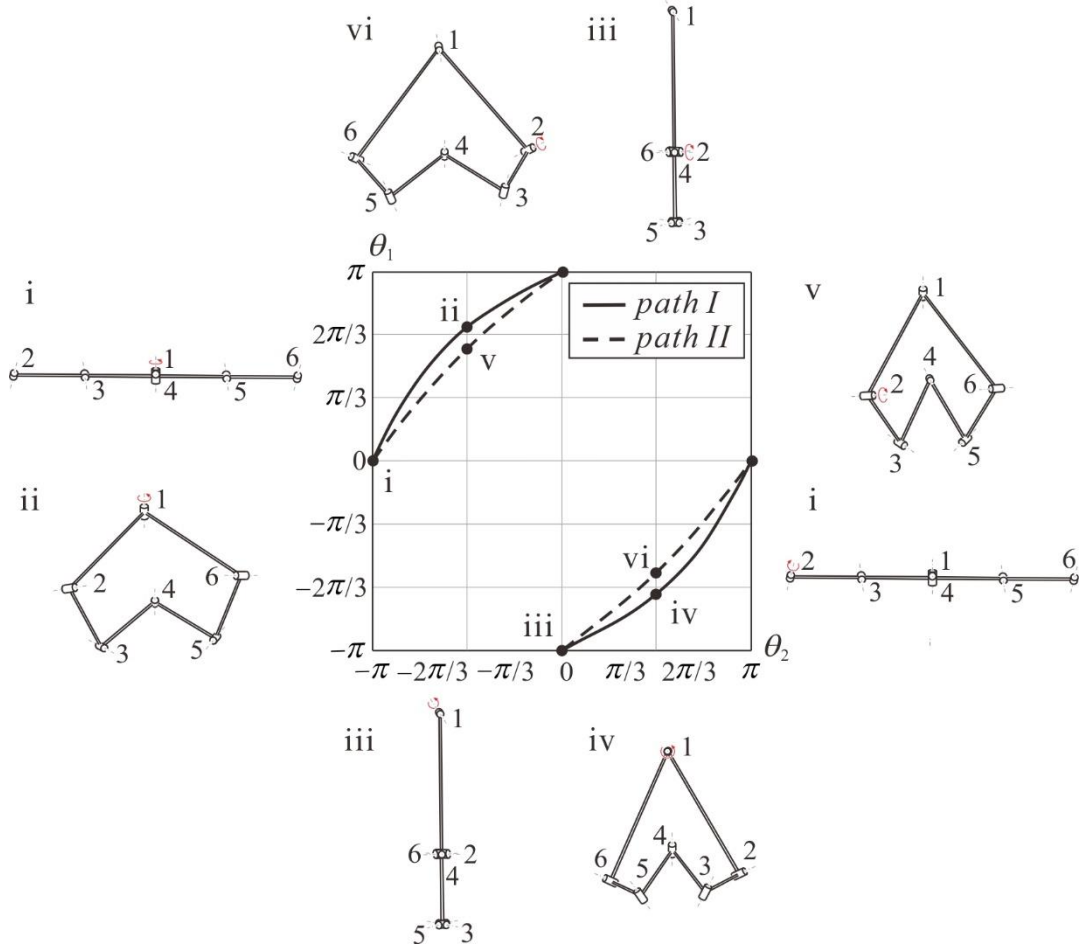


Fig. 6 Bifurcation between two 6R motion branches, where i-ii-iii-iv-i correspond to configurations of the linkage along *path I* and i-vi-iii-v-i correspond to configurations of the linkage along *path II*. Here the geometrical parameters of this linkage are  $a = 2, b = 1, c = 1, \alpha = \frac{2\pi}{3}, \beta = \frac{\pi}{6}, \gamma = -\frac{\pi}{6}, R_2 = R_3 = 0$ , which corresponds to Case 10 in Table 1.

It is found that Eq. (32a) and Eq. (32b) correspond to the cases that the linkage degenerates to a revolute joint, where links 12, 23 and 34 work as a whole part that rotates about joint 1 relative to the part consisting of links 45, 56 and 61. It is represented in Fig. 7a) as *path I* and *path III* respectively, where the joint 1 is chosen as the actuated joint highlighted with a rotation in red. Eq. (32c) corresponds to the case that the linkage degenerates to a serial kinematic chain with two revolute joints as shown in Fig. 7a) as *path II*, where there are two actuated joints 2 and 3. It should be noticed that there exists a case represented by Eq. (32d) that violates the plane-

symmetric motion shown as *path IV* along which configurations of the linkage are shown in Fig. 7b). The linkage is actually a four-bar double-rocker linkage.

The plotted paths define the values of two chosen kinematic variables at those selected points where corresponding configurations are presented, and other kinematic variables can be determined by other kinematic paths as well. Once all kinematic variables are given, configurations of the linkage at these points are definitely determined. The whole bifurcation behavior is presented in Fig. 7, where Fig. 7a) shows the bifurcation between two equivalent single-revolute-joint motion branches and a serial kinematic chain with two revolute joints, and Fig. 7b) shows the bifurcation between two equivalent single-revolute-joint motion branches and a four-bar double-rocker linkage motion branch.

## 6. Conclusions

In this paper, a thorough kinematic study of the general plane-symmetric Bricard linkage has been conducted. Based on the DH matrix method, the explicit solutions to closure equation of the plane-symmetric Bricard linkage have been derived first. Once the geometric condition is given, the kinematic relationship between different kinematic variables can be easily obtained. Even though Baker gave the implicit closure equations of a general plane-symmetric Bricard linkage [3], the explicit solutions provide a more effective way on kinematic and bifurcation analysis. Various cases of the plane-symmetric Bricard linkage with two, one or none  $6R$  kinematic paths have been compared. Moreover, the conditions to obtain degenerated  $5R/4R$  linkages from this kind of linkage have been elaborated.

Furthermore, various bifurcation cases of the plane-symmetric Bricard linkage with different geometric conditions, including the bifurcation between overconstrained  $6R$  and  $4R$  linkages, two  $6R$  linkages and among equivalent kinematic chains with single or double revolute joints and a four-bar double-rocker linkage, have been revealed. Especially, the bifurcation from the plane-symmetric Bricard linkage to the Bennett linkage has also been proposed. Normally, Bricard-related linkages and Bennett-based linkages [18] compose two major separated groups of single-loop overconstrained spatial linkages. This work further reveal the intrinsic relationship between these two groups after the proposal of the linkage reconfigurable between Bennett linkage and general line-symmetric Bricard linkage [19].

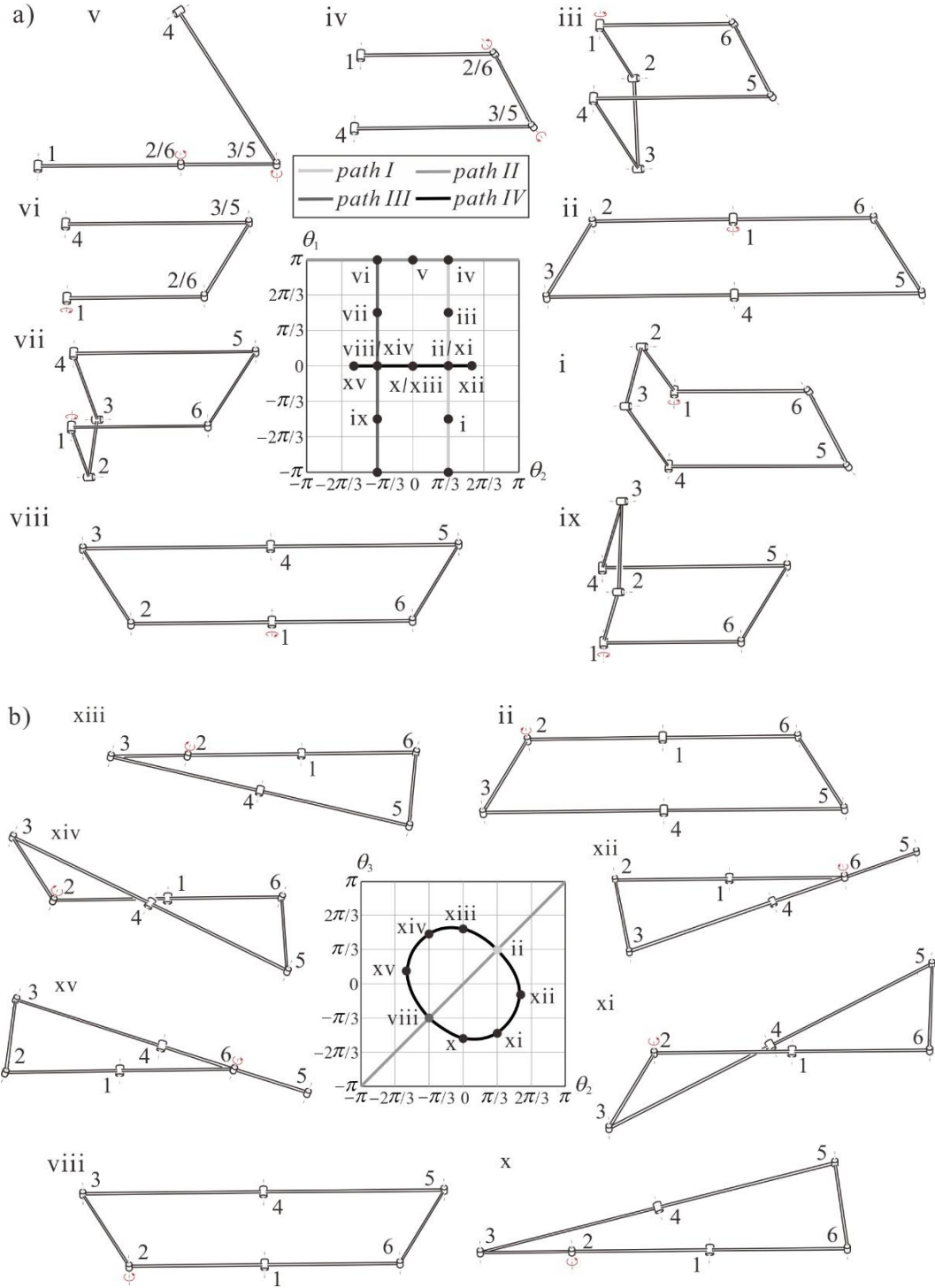


Fig. 7 Bifurcation of the plane-symmetric Bricard linkage: a) between equivalent single-revolute-joint branch and a serial kinematic chain with two revolute joints branch; b) between equivalent single-revolute-joint branch and a four-bar double-rocker linkage branch, where i-ii-iii-iv correspond to configurations of the linkage along *path I*, iv-v-vi correspond to configurations of the linkage along *path III*, vi-vii-viii-ix correspond to configurations of the linkage along *path II*, and viii-x-xi-xii-ii-xiii-xiv-xv correspond to configurations of the linkage along *path IV*.

Symmetry is usually adopted when we analyze the kinematics of deployable structures constructed by these basic overconstrained linkage elements. Based on the recent research on the thick-panel origami, the work in this paper not only offers an in-depth understanding about the kinematics of the general plane-symmetric Bricard linkage, but also establishes the essential mathematical foundation for extending origami patterns to practical engineering applications.

## Acknowledgments

H. Feng is grateful to the China Scholarship Council for the State Scholarship Fund and to Tianjin University for providing the University PhD Scholarship. The authors also acknowledge the support of the National Natural Science Foundation of China (Project No. 51275334, 51422506, 51290293 and 51535008) and the Ministry of Science and Technology of China (Project 2014DFA70710).

## Appendix

### A. Entries of closure equations of the plane-symmetric Bricard linkages

General case:

(1, 3):

$$\begin{aligned} & \sin \theta_1 (\cos \alpha \sin \gamma \sin \theta_2 \sin \theta_3 - \cos \alpha \cos \beta \sin \gamma \cos \theta_2 \cos \theta_3 + \sin \alpha \sin \beta \sin \gamma \cos \theta_3 \\ & - \cos \alpha \sin \beta \cos \gamma \cos \theta_2 - \sin \alpha \cos \beta \cos \gamma) = (1 + \cos \theta_1)(\sin \gamma \cos \theta_2 \sin \theta_3 \\ & + \cos \beta \sin \gamma \sin \theta_2 \cos \theta_3 + \sin \beta \cos \gamma \sin \theta_2) \end{aligned}$$

(1, 4):

$$\begin{aligned} & \sin \theta_1 [c(\cos \alpha \sin \theta_2 \cos \theta_3 + \cos \alpha \cos \beta \cos \theta_2 \sin \theta_3 - \sin \alpha \sin \beta \sin \theta_3) + b \cos \alpha \sin \theta_2 \\ & - R_3 \cos \alpha \sin \beta \cos \theta_2 - R_2 \sin \alpha - R_3 \sin \alpha \cos \beta] = (1 + \cos \theta_1)[c(\cos \theta_2 \cos \theta_3 \\ & - \cos \beta \sin \theta_2 \sin \theta_3) + b \cos \theta_2 + a + R_3 \sin \beta \sin \theta_2] \end{aligned}$$

(3, 1):

$$\begin{aligned} & (1 + \cos \theta_4)(\sin \alpha \sin \theta_2 \cos \theta_3 + \sin \alpha \cos \beta \cos \theta_2 \sin \theta_3 + \cos \alpha \sin \beta \sin \theta_3) \\ & = \sin \theta_4 [\cos \gamma (\sin \alpha \sin \theta_2 \sin \theta_3 - \sin \alpha \cos \beta \cos \theta_2 \cos \theta_3 - \cos \alpha \sin \beta \cos \theta_3) \\ & + \sin \gamma (\sin \alpha \sin \beta \cos \theta_2 - \cos \alpha \cos \beta)] \end{aligned}$$

When  $\theta_1 = \pi$ ,

(2, 3):

$$\begin{aligned} & \cos \alpha \sin \gamma \sin \theta_2 \sin \theta_3 - \cos \alpha \cos \beta \sin \gamma \cos \theta_2 \cos \theta_3 + \sin \alpha \sin \beta \sin \gamma \cos \theta_3 \\ & - \cos \alpha \sin \beta \cos \gamma \cos \theta_2 - \sin \alpha \cos \beta \cos \gamma = 0 \end{aligned}$$

(2, 4):

$$c(\cos \alpha \sin \theta_2 \cos \theta_3 + \cos \alpha \cos \beta \cos \theta_2 \sin \theta_3 - \sin \alpha \sin \beta \sin \theta_3) + b \cos \alpha \sin \theta_2 - R_3 \cos \alpha \sin \beta \cos \theta_2 - R_2 \sin \alpha - R_3 \sin \alpha \cos \beta = 0$$

When  $\theta_2 = \theta_6 = \pi$ ,

(1, 3):

$$\sin \theta_1 (\cos \alpha \cos \beta \sin \gamma \cos \theta_3 + \sin \alpha \sin \beta \sin \gamma \cos \theta_3 + \cos \alpha \sin \beta \cos \gamma - \sin \alpha \cos \beta \cos \gamma) = -\sin \gamma \sin \theta_3 (1 + \cos \theta_1)$$

(1, 4):

$$\sin \theta_1 [-c \cos \alpha \cos \beta \sin \theta_3 - c \sin \alpha \sin \beta \sin \theta_3 + R_3 \cos \alpha \sin \beta - R_2 \sin \alpha - R_3 \sin \alpha \cos \beta] = (1 + \cos \theta_1)(-c \cos \theta_3 - b + a)$$

When  $\theta_3 = \theta_5 = \pi$ ,

(1, 3):

$$\sin \theta_1 (\cos \alpha \cos \beta \sin \gamma \cos \theta_2 - \sin \alpha \sin \beta \sin \gamma - \cos \alpha \sin \beta \cos \gamma \cos \theta_2 - \sin \alpha \cos \beta \cos \gamma) = (1 + \cos \theta_1)(-\cos \beta \sin \gamma \sin \theta_2 + \sin \beta \cos \gamma \sin \theta_2)$$

(1, 4):

$$\sin \theta_1 [-c \cos \alpha \sin \theta_2 + b \cos \alpha \sin \theta_2 - R_3 \cos \alpha \sin \beta \cos \theta_2 - R_2 \sin \alpha - R_3 \sin \alpha \cos \beta] = (1 + \cos \theta_1)(-c \cos \theta_2 + b \cos \theta_2 + a + R_3 \sin \beta \sin \theta_2)$$

When  $\theta_4 = \pi$ ,

(1, 3):

$$\sin \theta_1 (\cos \alpha \sin \gamma \sin \theta_2 \sin \theta_3 - \cos \alpha \cos \beta \sin \gamma \cos \theta_2 \cos \theta_3 + \sin \alpha \sin \beta \sin \gamma \cos \theta_3 - \cos \alpha \sin \beta \cos \gamma \cos \theta_2 - \sin \alpha \cos \beta \cos \gamma) = (1 + \cos \theta_1)(\sin \gamma \cos \theta_2 \sin \theta_3 + \cos \beta \sin \gamma \sin \theta_2 \cos \theta_3 + \sin \beta \cos \gamma \sin \theta_2)$$

(1, 4):

$$\sin \theta_1 [c(\cos \alpha \sin \theta_2 \cos \theta_3 + \cos \alpha \cos \beta \cos \theta_2 \sin \theta_3 - \sin \alpha \sin \beta \sin \theta_3) + b \cos \alpha \sin \theta_2 - R_3 \cos \alpha \sin \beta \cos \theta_2 - R_2 \sin \alpha - R_3 \sin \alpha \cos \beta] = (1 + \cos \theta_1)[c(\cos \theta_2 \cos \theta_3 - \cos \beta \sin \theta_2 \sin \theta_3) + b \cos \theta_2 + a + R_3 \sin \beta \sin \theta_2]$$

(3, 2):

$$\cos \gamma (\sin \alpha \sin \theta_2 \sin \theta_3 - \sin \alpha \cos \beta \cos \theta_2 \cos \theta_3 - \cos \alpha \sin \beta \cos \theta_3) + \sin \gamma (\sin \alpha \sin \beta \cos \theta_2 - \cos \alpha \cos \beta) = 0$$

## B Definitions of some terms in the text

$$D = 2BC \sin \gamma \tan^2 \frac{\theta_2}{2} + 2(B^2 \sin(\beta + \gamma) + C^2 \sin(\beta - \gamma)) \tan \frac{\theta_2}{2} - 2BC \sin \gamma ,$$

$$E = -(B^2 \sin(\alpha - \beta - \gamma) + C^2 \sin(\alpha - \beta + \gamma)) \tan^2 \frac{\theta_2}{2} - 4BC \cos \alpha \sin \gamma \tan \frac{\theta_2}{2} , \\ -(B^2 \sin(\alpha + \beta + \gamma) + C^2 \sin(\alpha + \beta - \gamma))$$

$$F = 2BC \sin(\alpha - \beta) \tan^2 \frac{\theta_2}{2} + 2(B^2 - C^2) \sin \alpha \tan \frac{\theta_2}{2} - 2BC \sin(\alpha + \beta) ,$$

$$G = (B^2 \sin(\alpha - \beta - \gamma) - C^2 \sin(\alpha - \beta + \gamma)) \tan^2 \frac{\theta_2}{2} - 4BC \sin \alpha \cos \gamma \tan \frac{\theta_2}{2} , \\ -B^2 \sin(\alpha + \beta + \gamma) + C^2 \sin(\alpha + \beta - \gamma)$$

$$H = -2A \sin \gamma \tan^2 \frac{\theta_2}{2} - 2B \sin(\beta - \gamma) \tan \frac{\theta_2}{2} + 2A \sin \gamma ,$$

$$I = -B \pm \sqrt{B^2 - 4AC} ,$$

$$J = 4A \tan \frac{\theta_2}{2} (A \sin(\beta + \gamma) - C \sin(\beta - \gamma)) ,$$

$$K = B \sin(\alpha - \beta + \gamma) \tan^2 \frac{\theta_2}{2} + 4A \cos \alpha \sin \gamma \tan \frac{\theta_2}{2} + B \sin(\alpha + \beta - \gamma) ,$$

$$L = 2A((C \sin(\alpha - \beta + \gamma) - A \sin(\alpha - \beta - \gamma)) \tan^2 \frac{\theta_2}{2} + C \sin(\alpha + \beta - \gamma) - A \sin(\alpha + \beta + \gamma)) ,$$

$$M = -2A \sin(\alpha - \beta) \tan^2 \frac{\theta_2}{2} + 2B \sin \alpha \tan \frac{\theta_2}{2} + 2A \sin(\alpha + \beta) ,$$

$$N = 4A(A + C) \sin \alpha \tan \frac{\theta_2}{2} ,$$

$$O = B \sin(\alpha - \beta + \gamma) \tan^2 \frac{\theta_2}{2} + 4A \sin \alpha \cos \gamma \tan \frac{\theta_2}{2} - B \sin(\alpha + \beta - \gamma) ,$$

$$P = 2A((C \sin(\alpha - \beta + \gamma) + A \sin(\alpha - \beta - \gamma)) \tan^2 \frac{\theta_2}{2} - C \sin(\alpha + \beta - \gamma) - A \sin(\alpha + \beta + \gamma)) .$$



## References

- [1] R. Bricard, Mémoire sur la théorie de l'octaèdre articulé, *Journal de Mathématiques Pures et Appliquées*, Liouville, 3, 1897, pp. 113–148.
- [2] R. Bricard, *Leçons de cinématique*, Tome II Cinématique Appliquée, Gauthier-Villars, Paris, 1927, pp. 7–12.
- [3] J.E. Baker, An analysis of Bricard linkages, *Mechanism and machine Theory*, 15, 1980, pp. 267–286.
- [4] J. Phillips, *Freedom in Machinery II: Screw Theory Exemplified*, Cambridge University Press, Cambridge, UK, 1990.
- [5] J. E. Baker, The single screw reciprocal to the general plane-symmetric six-screw linkage, *J. Geometry Graphics*, 1(1), 1997, pp. 5–12.
- [6] Z. Li, J. Schicho, A technique for deriving equational conditions on the Denavit–Hartenberg parameters of  $6R$  linkages that are necessary for movability, *Mechanism and Machine Theory*, 94, 2015, pp. 1–8.
- [7] Z. Deng, H. Huang, B. Li, R. Liu, Synthesis of deployable/foldable single loop mechanisms with revolute joints, *Journal of Mechanisms and Robotics*, 3(3), 2011, pp. 031006.
- [8] H. Huang, Z. Deng, X. Qi, B. Li, Virtual chain approach for mobility analysis of multiloop deployable mechanisms, *Journal of Mechanical Design*, 135(11), 2013, pp. 111002.
- [9] X. Kong, Type synthesis of single-loop overconstrained  $6R$  spatial mechanisms for circular translation, *Journal of Mechanisms and Robotics*, 6(4), 2014, pp. 041016.
- [10] Y. Chen, Z. You, T. Tarnai, Threefold-symmetric Bricard linkages for deployable structures, *International Journal of Solids and Structures*, 42 (8), 2005, pp. 2287–2301.
- [11] A D. Viquerat, T. Hutt, S D. Guest, A plane symmetric  $6R$  foldable ring, *Mechanism and Machine Theory*, 63, 2013, pp. 73–88.
- [12] X. Qi, H. Huang, Z. Miao, B. Li, Z. Deng, Design and mobility analysis of large deployable mechanisms based on plane-symmetric Bricard linkage, *Journal of Mechanical Design*, 139(2), 2017, pp. 022302.
- [13] Y. Chen, W.H. Chai, Bifurcation of a special line and plane symmetric Bricard linkage, *Mechanism and Machine Theory*, 46(4), 2011, pp. 515–533.
- [14] K. Zhang, J.S. Dai, Geometric constraints and motion branch variations for reconfiguration of single-loop linkages with mobility one, *Mechanism and Machine Theory*, 106, 2016, pp. 16–29.
- [15] Y. Chen, R. Peng, Z. You, Origami of thick panels, *Science*, 349(6246), 2015, pp. 396–400.
- [16] Y. Chen, H. Feng, J. Ma, R. Peng, Z. You, Symmetric waterbomb origami, *Proceedings of the Royal Society A*, 472(2190), 2016, pp. 20150846.
- [17] J. Denavit, R.S. Hartenberg, A kinematic notation for lower-pair mechanisms based on matrices, *Transactions of the ASME: Journal of Applied Mechanics*, 23, 1955, pp. 215–221.
- [18] J.E. Baker, A comparative survey of the Bennett-based, 6-revolute kinematic loops, *Mechanism and Machine Theory*, 28, 1993, pp. 83–96.
- [19] C. Y. Song, Y. Chen, I. M. Chen, A  $6R$  linkage reconfigurable between the line-symmetric Bricard linkage and the Bennett linkage, *Mechanism and Machine Theory*, 70, 2013, pp. 278–292.